ACS OMEGA

http://pubs.acs.org/journal/acsodf

Article

Functionalization of Silica Nanoparticles by 5-Chloro-8-quinolinol as a New Nanocomposite for the Efficient Removal and Preconcentration of Al^{3+} Ions from Water Samples

Asma S. Al-Wasidi, Hanadi A. Katouah, Fawaz A. Saad, and Ehab A. Abdelrahman*

Cite This: *ACS Omega* 2023, 8, 15276−15287

Read Online

ACCESS | Metrics & More | Article Recommendations | Supporting Information

ABSTRACT: In this work, silica nanoparticles were modified by 5-chloro-8-quinolinol as a new nanocomposite for the efficient elimination and preconcentration of Al^{3+} ions from several water sources. The fabricated composite was characterized utilizing XRD, SEM, FT-IR, TEM, CHN elemental analyzer, and N_2 adsorption/desorption analyzer. The XRD demonstrated the existence of a wide peak at $2\theta = 30°$. Also, all the peaks of silica were severely reduced, which confirms the success of loading the 5-chloro-8-quinolinol on the surface of the silica. The SEM and TEM images demonstrated that the composite resembled cotton, and this confirms that 5-chloro-8-quinolinol was successfully loaded on the silica surface. The specific surface area, the average pore size, and the total pore volume of the synthesized composite are 80.53 m^2/g, 3.26 nm, and 0.185 cc/g, respectively. In addition, the greatest uptake capacity of the synthesized composite toward aluminum ions is 95.06 mg/g. The results indicated that the adsorption of aluminum ions onto the silica/5-chloro-8-quinolinol composite follows the Langmuir isotherm and pseudo-second-order model. Moreover, the adsorption of aluminum ions by the silica/5-chloro-8-quinolinol composite is spontaneous, chemical, and thermodynamically favorable. The values of % recovery were more than 97%, whereas the values of % RSD were less than 3.5%. Hence, this confirms the effectiveness of the proposed method in the determination of aluminum ions in real water samples.

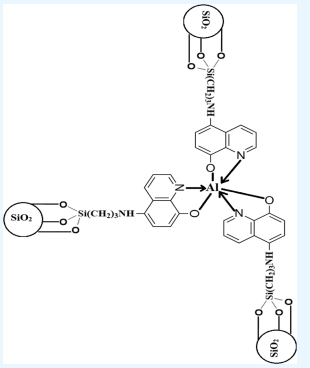

1. INTRODUCTION

Human activities, industrial wastes, and mining operations have recently contributed to an increase in the contamination of water, soil, and the environment with several metals.[1,2] Aluminum metal is regarded to be a plentiful element in the earth's crust, but it is also a non-essential and toxic element to which humans are exposed through dust, air, food, water, and the consumption of medications and cosmetics.[3] Owing to the usage of the aluminum compounds as coagulants in the field of water treatment, the level of aluminum in drinking water may be increased. Principal organs influenced by aluminum poisoning are the bones, central nervous system, and lungs. Alzheimer's and osteomalacia diseases are the most prevalent disorders resulting from overexposure to aluminum.[4] According to the World Health Organization, the level of aluminum in water is between 0.001 and 0.05 mg/L. According to the United States Environmental Protection Agency, the secondary significant contaminant limit for the aluminum in drinking water is between 0.05 and 0.20 mg/L.[5] Therefore, it is essential for removing aluminum from the sources of water. Irrespective of the recognition technique, the assessment of trace amounts of metals requires preconcentration and separation processes to eliminate interfering influences and ensure that the analyte concentration is quantifiable. In the literature, various procedures for extraction and preconcentration of aluminum prior to analysis, such as liquid−liquid extraction, co-precipitation, single-drop microextraction, cloud point extraction, and solid-phase removal, have been defined.[6−9] Solid-phase removal was employed for the extraction of numerous kinds of contaminants from aqueous solutions since it provides many advantages, such as easy operation, high selectivity, cheap cost, minimal time, and the ability to be combined with various modern detection techniques.[10] Recently, some adsorbents were used for the removal and preconcentration of aluminum ions from aqueous solutions, such as Linde type-A zeolite, magnetic activated carbon/tungsten nanocomposite, iron-modified activated carbons, cellulose modified with gallic acid, montmorillonite, spent mushroom substrate, functional graphene materials, bio-sorbents derived from the stems of plants, activated carbon, natural zeolite, and polymeric resins.[11−18] In recent years, the fabrication of eco-friendly and green adsorbents with high separation capacities for harmful metal ions has posed a significant challenge to the control of environmental pollution.[19−22] In this regard, Bulgariu and Bulgariu synthesized a novel adsorbent via the

Received: January 20, 2023
Accepted: April 10, 2023
Published: April 19, 2023

functionalization of soy waste biomass by an industrial sulfur-based chelating agent for the removal of Pb(II), Cu(II), and Ni(II) ions from aqueous media.[23] Nowadays, silica is a widely utilized adsorbent with multiple uses in separation processes. Numerous advantages of silica include its high activity, high adsorption capacity, ease of preparation, diverse pore diameters and surface areas, and the potential for surface functionalization.[24,25] The utilization of silane as a coupling agent to modify the surface of nanoparticles, such as alumina and silica, has been the subject of a large number of recent studies.[26,27] By combining various functional groups with the surface of silica, it has been shown that the adsorption behavior can be altered and applicable on a large scale. A vast variety of organic compounds, such as dibenzoylmethane and 4,6-diacetylresorcinol, capable of chelating with a series of metal ions were used to functionalize the surface of silica.[24,25] Today, solid-phase removal utilizing nanostructures is regarded as a clean adsorptive method that protects humans from the harmful environmental effects of trace amounts of heavy metals and enhances their reusability and recovery. Once coupled with solid-phase extraction, nanomaterial's high surface areas and strong uptake capacities result in enhanced performance for the preconcentration of trace heavy metals. Due to the above information, the objective of this study was the facile modification of silica nanoparticles with 5-chloro-8-quinolinol as a new composite for efficient elimination and preconcentration of aluminum ions from water sources. The reason for using 5-chloro-8-quinolinol is that it contains a hydroxyl group and a nitrogen atom that have the ability to form five-ring chelates with several metal ions. Consequently, it is expected that this substance will be effective in the field of treatment and assessment of pollutants. According to our review of the relevant literature, the novelty of this study lies in the fact that the fabricated composite was not previously used as an adsorbent for the removal of aluminum ions from aqueous media as well as its great adsorption capacity due to its ability to form chelate coordination compounds with the aluminum ions. The formed composite was identified using XRD, CHN elemental analyzer, FT-IR, TEM, SEM, and BET analyses. Using batch experiments, the effect of several parameters that affect the adsorption process was investigated and adjusted. Various isotherm models were used to analyze equilibrium data. In order to comprehend the adsorption mechanism of aluminum ions on fabricated composite, kinetic and thermodynamic investigations were conducted.

2. EXPERIMENTAL SECTION

2.1. Materials and Reagents. 5-Chloro-8-quinolinol (C_9H_6ClNO), hydrochloric acid (HCl), potassium nitrate (KNO_3), (3-aminopropyl)trimethoxysilane ($C_6H_{17}NO_3Si$), diethyl ether ($C_4H_{10}O$), sodium metasilicate pentahydrate ($Na_2SiO_3{\cdot}5H_2O$), cetyltrimethylammonium bromide ($C_{19}H_{42}BrN$), nitric acid (HNO_3), thiourea (CH_4N_2S), ethanol (C_2H_6O), sodium hydroxide (NaOH), xylene (C_8H_{10}), ethylenediaminetetraacetic acid disodium salt dihydrate ($C_{10}H_{16}N_2Na_4O_{10}$), and aluminum(III) chloride hexahydrate ($AlCl_3{\cdot}6H_2O$) were purchased from Merck Chemical Company (Purity equals 99.99%) and used without any refinement.

2.2. Fabrication of the Silica/5-Chloro-8-quinolinol Composite. Initially, the silica/(3-aminopropyl)-trimethoxysilane composite was produced by exploiting the procedure reported by Al-Wasidi et al.[25] Afterward, 2.80 g of the silica/(3-aminopropyl)trimethoxysilane composite was added to a 120 mL ethanolic solution containing 2.80 g of 5-chloro-8-quinolinol and then refluxed with stirring for about 24 h. Finally, the silica/5-chloro-8-quinolinol composite was pump filtered, carefully washed using ethanol, water, and diethyl ether, and dried at 55 °C.

2.3. Instrumentation. The concentration of aluminum ions was determined by flame atomic absorption spectrometry (GBC& SensAA Series) at a wavelength equals 309.30 nm. Using a Nicolet FT-IR spectrometer in the range from 4000 to 400 cm^{-1}, functional groups located on the surface of the silica/5-chloro-8-quinolinol composite were identified. Utilizing scanning electron microscopy (JEOL & SEM-JSM-5410LV) and transmission electron microscopy (JEOL 2010), the morphology of the silica/5-chloro-8-quinolinol composite was evaluated. The X-ray diffraction (XRD) pattern of the silica/5-chloro-8-quinolinol composite was recorded on X-ray diffractometer (Bruker & D8 Advance). Utilizing a surface area analyzer (Quantachrome & NOVA), the surface area of the silica/5-chloro-8-quinolinol composite was determined. A CHN Elemental Analyzer (PerkinElmer) was utilized for the determination of the CHN precent of the silica/5-chloro-8-quinolinol composite.

2.4. Removal of Al^{3+} Ions from the Aqueous Solutions. *2.4.1. Effect of pH.* For studying the effect of pH in the variation interval from 2 to 6, using 250 mL conical flasks, 0.06 g of the silica/5-chloro-8-quinolinol nanocomposite was blended with 60 mL of about 120 mg/L of Al^{3+} aqueous solution. Then, the pH of the aluminum solution was adjusted using 0.1 M HCl and/or NaOH. All the flasks have been stirred at 550 rpm for 3 h.

2.4.2. Effect of Time. For studying the effect of time in the variation interval from 10 to 120 min, using 250 mL conical flasks, 0.06 g of the silica/5-chloro-8-quinolinol nanocomposite was blended with 60 mL of about 120 mg/L of Al^{3+} aqueous solution. Then, the pH of the aluminum solution was adjusted to about 6. All the flasks have been stirred at 550 rpm.

2.4.3. Effect of Temperature. For studying the effect of temperature in the variation interval from 298 to 328 K, using 250 mL conical flasks, 0.06 g of the silica/5-chloro-8-quinolinol nanocomposite was blended with 60 mL of about 120 mg/L of Al^{3+} aqueous solution. Then, the pH of the aluminum solution was adjusted to about 6. All the flasks have been stirred at 550 rpm for 60 min.

2.4.4. Effect of Concentration. For studying the effect of aluminum concentration in the variation interval from 40 to 160 mg/L, using 250 mL conical flasks, 0.06 g of the silica/5-chloro-8-quinolinol nanocomposite was blended with 60 mL of 40−160 mg/L of Al^{3+} aqueous solution. Then, the pH of the aluminum solution was adjusted to about 6. All the flasks have been stirred at 550 rpm for 60 min.

After the completion of any of the aforementioned effects, the adsorbent is separated using a centrifuge, and the aluminum concentration is estimated in the filtrate using flame atomic absorption spectrometry. The mass of eliminated Al^{3+} ions per gram of the silica/5-chloro-8-quinolinol nanocomposite (Q, mg/g) can be calculated by eq 1.

$$Q = [C_i - C_e] \times V/M \quad (1)$$

The % removal of Al^{3+} ions (% R) can be calculated using eq 2.

$$\%R = ((C_i - C_e)/C_i) \times 100 \quad (2)$$

https://doi.org/10.1021/acsomega.3c00413
ACS Omega 2023, 8, 15276−15287

where C_i represents the initial concentration of Al^{3+} ions prior to adsorption (mg/L), whereas C_e represents the concentration of Al^{3+} ions in the filtrate after adsorption (mg/L). V is the volume of Al^{3+} solution (L), whereas M is the quantity of the silica/5-chloro-8-quinolinol composite (g).

Scheme 1. Synthesis of the Silica/5-Chloro-8-quinolinol Composite

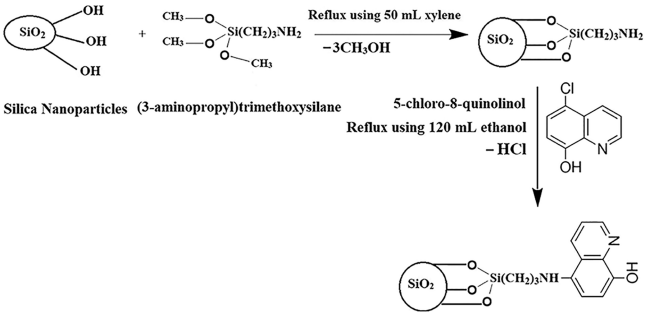

2.4.5. Effect of Desorption and Reusability. For the desorption investigation, 0.06 g of the silica/5-chloro-8-quinolinol nanocomposite was blended with 60 mL of 5 mg/L of Al^{3+} solution then stirred for 60 min at temperature = 25 °C and pH = 6. The loaded composite with Al^{3+} ions was separated, washed carefully by distilled water, and dried at 50 °C. After that, the loaded composite was blended with 4.00 mL of about 0.40 M of certain eluting solutions (nitric acid, thiourea, EDTA disodium salt, and hydrochloric acid) and then stirred at 550 rpm for 15 min. To test reusability studies for about four adsorption/desorption cycles, 0.06 g of the recovered adsorbent was magnetically stirred for 60 min with 5 mg/L of Al^{3+} solution at pH = 6. Notably, 0.40 M EDTA disodium salt is used to regenerate the adsorbent after each cycle. In addition, eq 3 can be exploited to get the percentage of desorption (% D).

$$\%D = (100C_d \times V_d)/((C_i - C_e) \times V) \quad (3)$$

where C_d is the concentration of Al^{3+} ions that exist in the eluting solution (mg/L), whereas V_d is the volume of eluting solution (L).

2.4.6. Point of Zero Charge of the Silica/5-Chloro-8-quinolinol Composite. According to Al-Wasidi et al.,[25] the point of zero charge (pH_{PZC}) of the silica/5-chloro-8-quinolinol composite can be obtained as follows: Exploiting 0.1 M HCl or NaOH, the initial pH of 0.03 M potassium nitrate solutions was altered to different values in the variation interval from 2.0 to 12.0. Then, 0.15 g of the silica/5-chloro-8-quinolinol nanocomposite was mixed with any potassium nitrate solution and stirred for 8 h. The silica/5-chloro-8-quinolinol composite was carefully separated by centrifugation, and the final pH value of the filtrate was estimated. In a graph, the final pH values were plotted against initial pH values. The

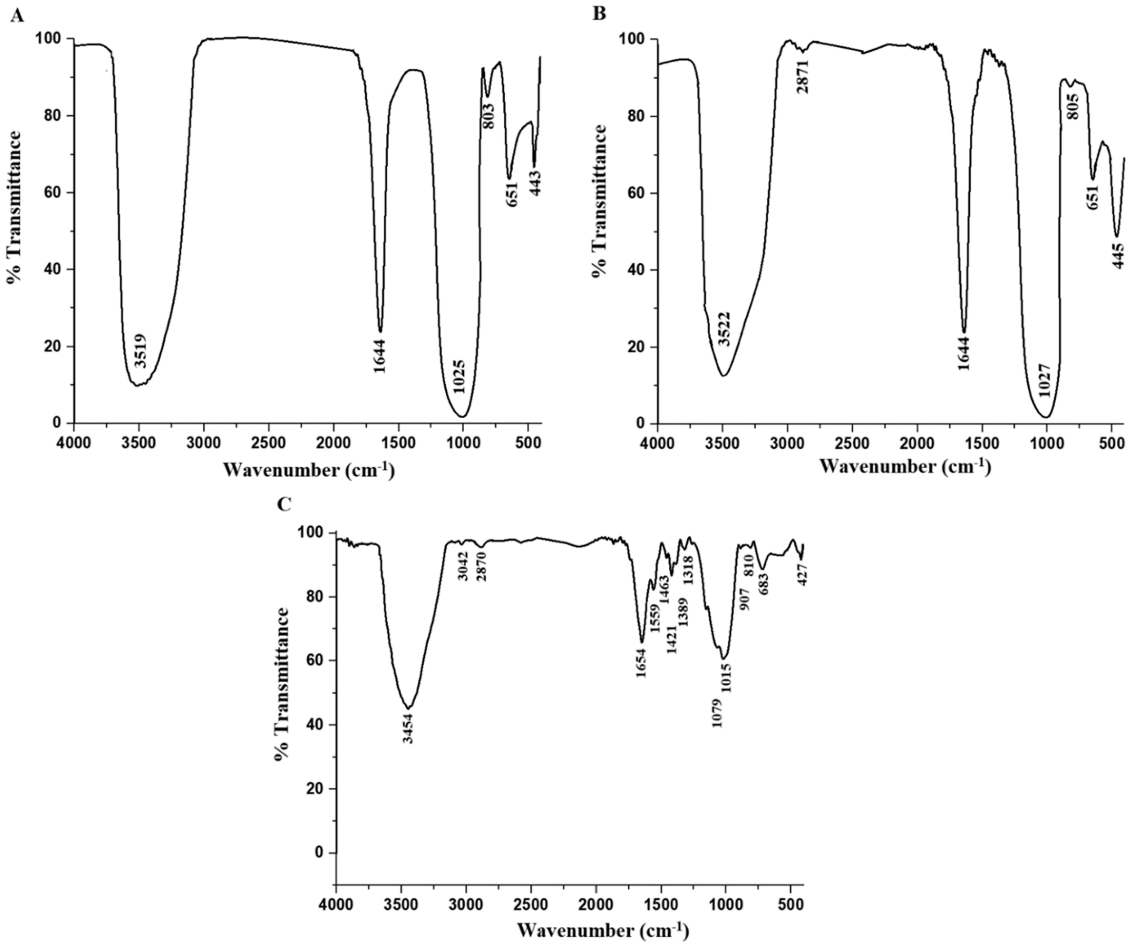

Figure 1. FT-IR spectrum of the silica (A), silica/(3-aminopropyl)trimethoxysilane composite (B), and silica/5-chloro-8-quinolinol composite (C).

https://doi.org/10.1021/acsomega.3c00413
ACS Omega 2023, 8, 15276−15287

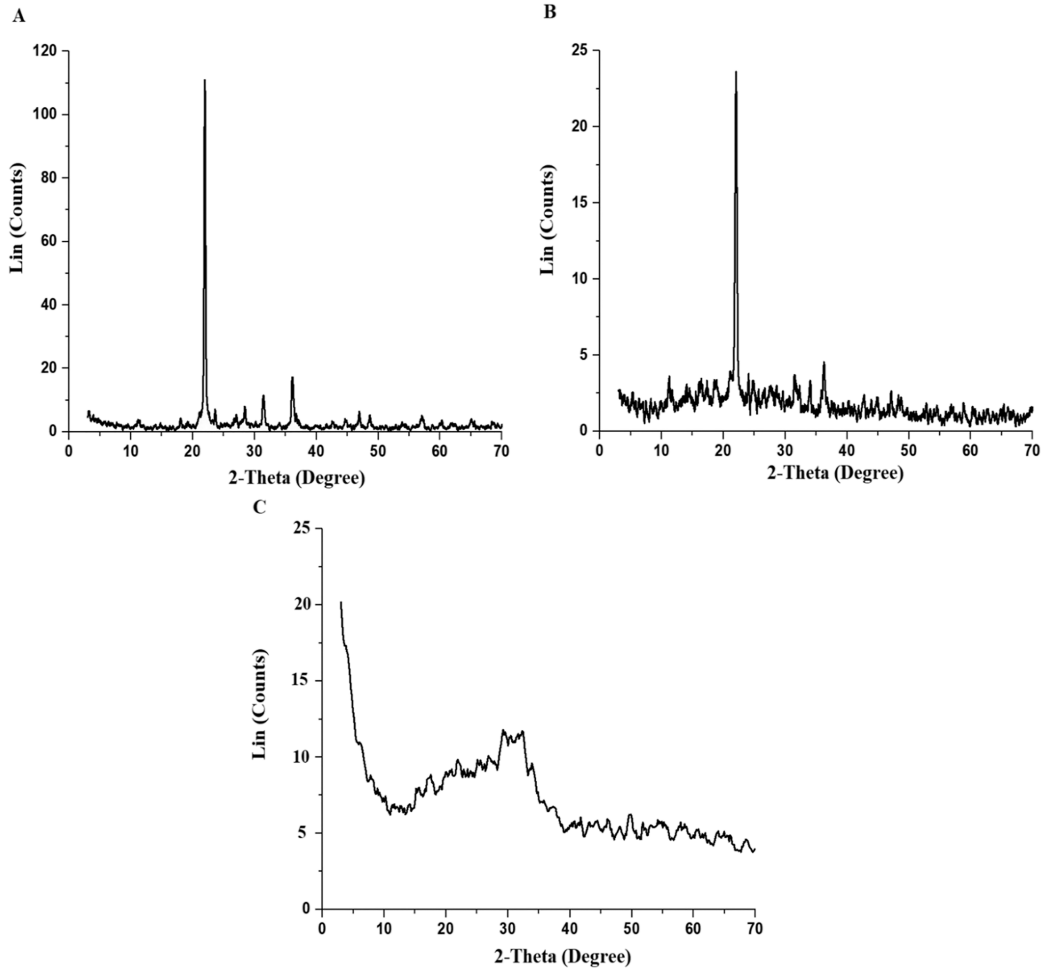

Figure 2. XRD patterns of the silica (A), silica/(3-aminopropyl)trimethoxysilane composite (B), and silica/5-chloro-8-quinolinol composite (C).

pH_{pzc} is the final pH at which a characteristic plateau was reached.[24]

2.4.7. Determination of Aluminum Ions in Real Water Samples. Real water samples were gathered from different places in Egypt (Alexandria, Ras El-Bar, and Gamasah), at a 50 cm depth from the level of surface water. Additionally, all the water samples were then filtered and stored in polyethylene bottles at 5 °C in the refrigerator for future use. Aluminum ions were separated from real water samples then concentrated under optimum conditions which were previously explained in the adsorption and desorption parts. Also, Al^{3+} concentrations were added to collected real water samples and the application of the produced composite for the removal of Al^{3+} ions was assessed.

3. RESULTS AND DISCUSSION

3.1. Characterization of the Silica/5-Chloro-8-quinolinol Composite. *3.1.1. Elemental Analysis.* The obtained results of the elemental analysis for the silica/5-chloro-8-quinolinol composite showed that % C, % H, and % N are 20.35, 3.42, and 1.89%, respectively. In addition, the presence of carbon, hydrogen, and nitrogen after the encapsulation of 5-chloro-8-quinolinol on the surface of silica nanoparticles is a direct indication of the success of the encapsulation process as clarified in Scheme 1.

3.1.2. FT-IR. Figure 1A−C represents the FT-IR spectra of the silica, silica/(3-aminopropyl)trimethoxysilane composite, and silica/5-chloro-8-quinolinol composite, respectively. In addition, the bands at 443, 445, and 427 cm^{-1} are because of the bending vibration of O−Si−O. The bands at 651, 803, 805, and 810 cm^{-1} are owing to the symmetrical stretching vibration of Si−O−Si. The bands at 1025, 1027, and 1079 cm^{-1} are because of the asymmetrical stretching vibration of Si−O−Si. The bands at 1644 and 1654 cm^{-1} are because of the bending vibration of the OH and/or NH group. The bands at 3519, 3522, and 3454 cm^{-1} are because of the stretching vibration of OH and/or NH. Several organic groups appeared in the FT-IR analysis of the silica/5-chloro-8-quinolinol composite, confirming the success of the functionalization of silica nanoparticles with 5-chloro-8-quinolinol as clarified in Scheme 1. Amine groups are good nucleophiles, which reacts with the chloride group of 5-chloro-8-quinolinol where HCl is evolved, and the composite is formed as clarified in Scheme 1. This behavior has been observed previously with other related materials as reported by Cui et al.[28] and Fan et al.[29] In this regard, the bands centered at 3042 and 2870 cm^{-1} are because of the stretching vibration of the aromatic and aliphatic CH, respectively. In addition, the bands centered at 1389, 1421, 1463, and 1559 cm^{-1} are because of the stretching vibrations of C=C aromatic. In addition, the band centered at 1318 cm^{-1} is because of the bending vibration of CH. The bands at 907 and 1015 cm^{-1} are because of the out-of-plane bending vibration of aromatic CH.[25,30,31] According to the presented findings, FT-IR demonstrated that silica nanoparticles were

https://doi.org/10.1021/acsomega.3c00413
ACS Omega 2023, 8, 15276−15287

successfully modified with 5-chloro-8-quinolinol as clarified in Scheme 1.

3.1.3. X-ray Diffraction. Figure 2 represents the XRD patterns of the silica, silica/(3-aminopropyl)trimethoxysilane composite, and silica/5-chloro-8-quinolinol composite, respectively. The results confirmed the existence of a wide peak at $2\theta = 30°$ in the case of silica/5-chloro-8-quinolinol composite. All the peaks of silica were severely reduced, which confirms the success of loading the 5-chloro-8-quinolinol on the surface of the silica as clarified in Scheme 1 because the organic materials tend to be amorphous.[1] This behavior has been observed previously with other related materials as reported by Kenawy et al.[32]

3.1.4. SEM and TEM. Figure 3A,B represents the SEM images of the SiO_2 and silica/5-chloro-8-quinolinol nanocomposite, respectively. Also, Figure 3C,D represents the TEM images of the SiO_2 and silica/5-chloro-8-quinolinol nanocomposite, respectively. In addition, the results demonstrated that the SiO_2 consists of sphere and irregular particles. Moreover, the results demonstrated that the silica/5-chloro-8-quinolinol composite resembled cotton and this confirms that 5-chloro-8-quinolinol was successfully loaded on the surface of the synthesized silica as clarified in Scheme 1 because the organic materials tend to be amorphous.[1] This behavior has been observed previously with other related materials as reported by Kenawy et al.[32]

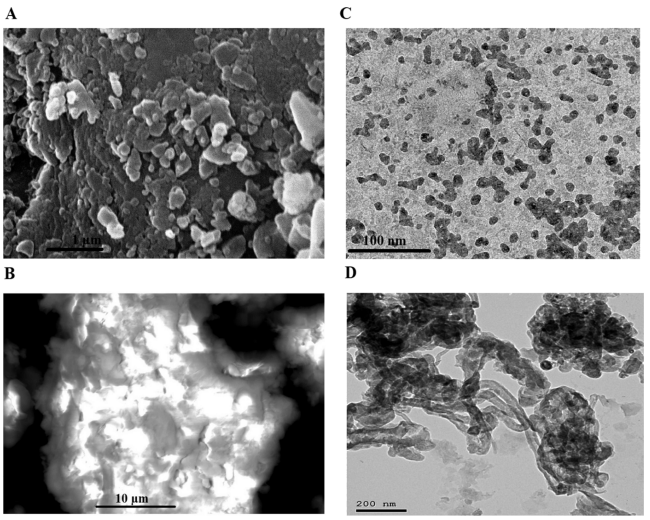

Figure 3. SEM images of SiO_2 (A) and silica/5-chloro-8-quinolinol composite (B). The TEM images of SiO_2 (C) and silica/5-chloro-8-quinolinol composite (D).

3.1.5. Surface Textures. The Brunauer−Emmett−Teller method was used to determine the specific surface area, the average pore size, and the total pore volume of the silica/5-chloro-8-quinolinol composite. The specific surface area, the average pore size, and the total pore volume of the composite are 80.53 m^2/g, 3.26 nm, and 0.185 cc/g, respectively. The noticeable decrease in the surface area of the composite compared to silica confirms the success of loading 5-chloro-8-quinolinol onto the silica surface as clarified in Scheme 1.[25]

3.2. Removal of Al^{3+} Ions from the Aqueous Solutions. *3.2.1. Influence of pH.* The values of removal efficiency (% *R*) and adsorption capacity (*Q*) increased when the pH value increased from 2 to 6, as shown in Figure 4A,B, respectively. % *R* and *Q* (mg/g) values at pH = 6 are 74.52% and 89.42 mg/g, respectively. The effects of pH values greater than 6 have not been studied because of the precipitation of Al^{3+} ions at those levels.

Plotting the final and initial values of pH of KNO_3 solutions in the presence of the composite prove that the value of point of zero charge of the nanocomposite is 2.95, as shown in Figure 5. Placing the silica/5-chloro-8-quinolinol composite in a medium that has a pH value less than the point of zero charge (2.95) causes the surface to be surrounded by the positive hydrogen ions that repel Al^{3+} ions, thus reducing the separation efficiency and adsorption capacity.[25] Placing the silica/5-chloro-8-quinolinol composite in a medium that has a pH value greater than the point of zero charge (2.95) causes the surface to be surrounded by the negative hydroxide ions that attract Al^{3+} ions and ionize the OH group of the organic substance, thus increasing the separation efficiency and adsorption capacity.[24,25] Therefore, pH = 6 is the best value at which the maximum possible amount of aluminum ions can be removed. The removal mechanism diagram of modified nanoparticles for aluminum ions from water and food samples is illustrated in Scheme 2.

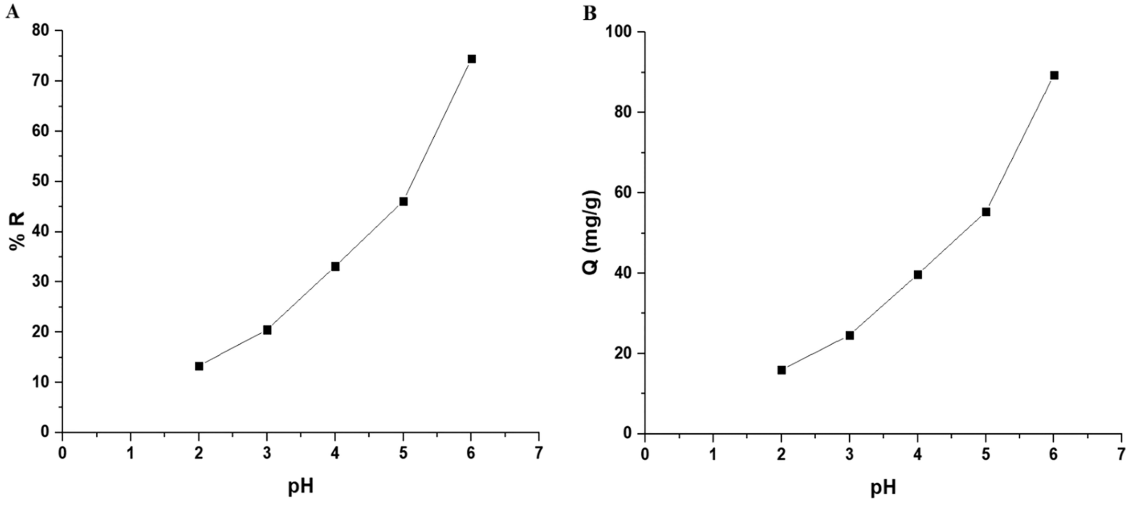

Figure 4. Effect of pH on % *R* (A) and adsorption capacity (B).

https://doi.org/10.1021/acsomega.3c00413
ACS Omega 2023, 8, 15276−15287

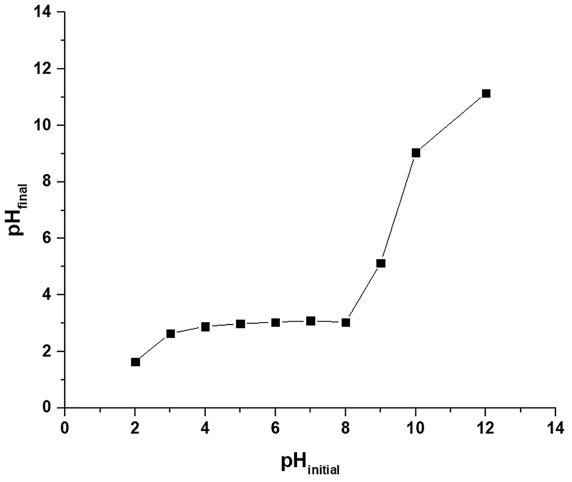

Figure 5. Point of zero charge of the silica/5-chloro-8-quinolinol composite.

Scheme 2. Mechanism of the Removal of Al^{3+} Ions Using the Synthesized Composite

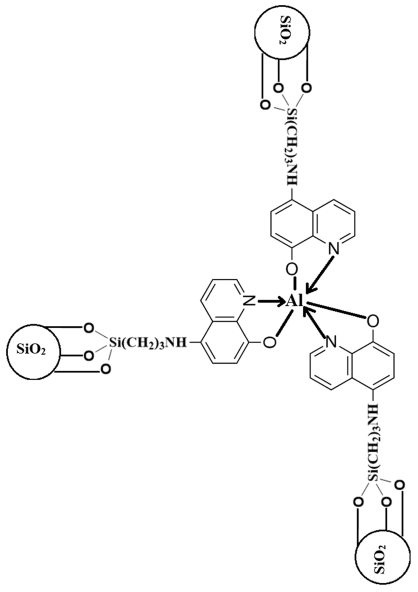

3.2.2. Influence of Contact Time. The values of removal efficiency (% R) and adsorption capacity (Q) increased when the contact time value increased from 10 to 60 min, as shown in Figure 6A,B, respectively. % R and Q (mg/g) values at time = 60 min are 75.00% and 90.00 mg/g, respectively. It was also noted that the values of the removal efficiency and adsorption capacity are almost constant when the time is increased from 60 to 120 min. Therefore, time = 60 min is the best value at which the maximum possible amount of aluminum ions can be removed.

To study the significant step of the uptake process, experimental results were fitted with pseudo-second-order and pseudo-first-order models, which are described by eqs 4 and 5, respectively.

$$\frac{t}{Q_t} = \frac{1}{K_2 Q_e^{\,2}} + \frac{1}{Q_e} t \tag{4}$$

$$\log(Q_e - Q_t) = \log Q_e - \frac{K_1}{2.303} t \tag{5}$$

where Q_e is the uptake capacity of the silica/5-chloro-8-quinolinol composite (mg/g) at equilibrium. Q_t (mg/g) is the adsorption capacity of the silica/5-chloro-8-quinolinol composite (mg/g) at time t. K_1 is the rate constant of the pseudo-first-order model (1/min), whereas K_2 is the rate constant of the pseudo-second-order model (g/mg min). Figure 7A,B displays the pseudo-first-order and pseudo-second-order models, respectively. The constants of the pseudo-first-order and pseudo-second-order models, as well as their correlation coefficient R^2 values, are tabulated in Table 1.

The preceding results indicated that the adsorption of aluminum ions onto the silica/5-chloro-8-quinolinol composite follows the pseudo-second-order model due to the following reasons: (1) The value of correlation coefficient (R^2) of the pseudo-second-order model is more than that of the pseudo-first-order model. (2) The value of Q_e predicted by the pseudo-second-order model corresponds more closely to the experimental data than the value of Q_e predicated by the pseudo-first-order model. Hence, there is a powerful force between the silica/5-chloro-8-quinolinol composite and aluminum ions due to the complexation of aluminum ions

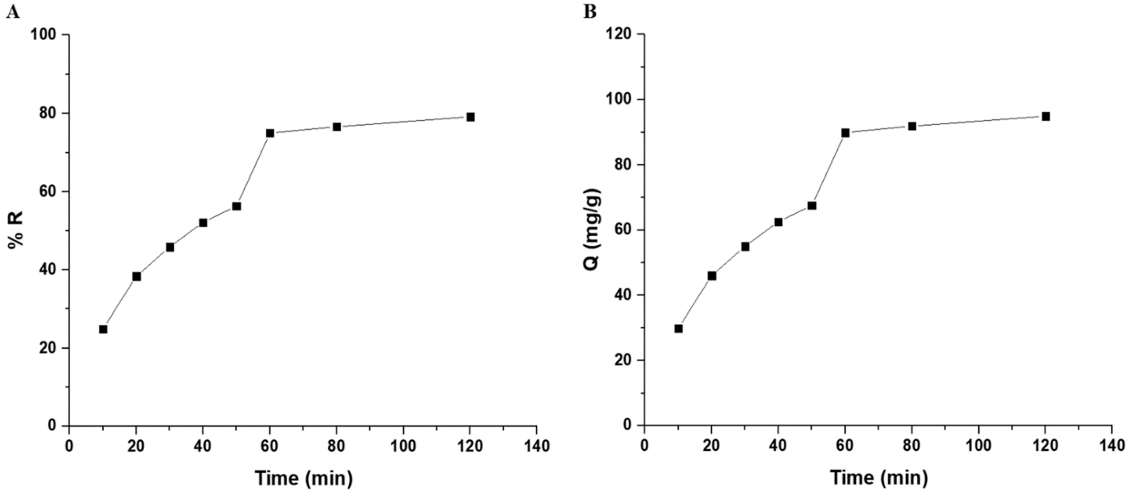

Figure 6. Effect of time on % R (A) and adsorption capacity (B).

https://doi.org/10.1021/acsomega.3c00413
ACS Omega 2023, 8, 15276−15287

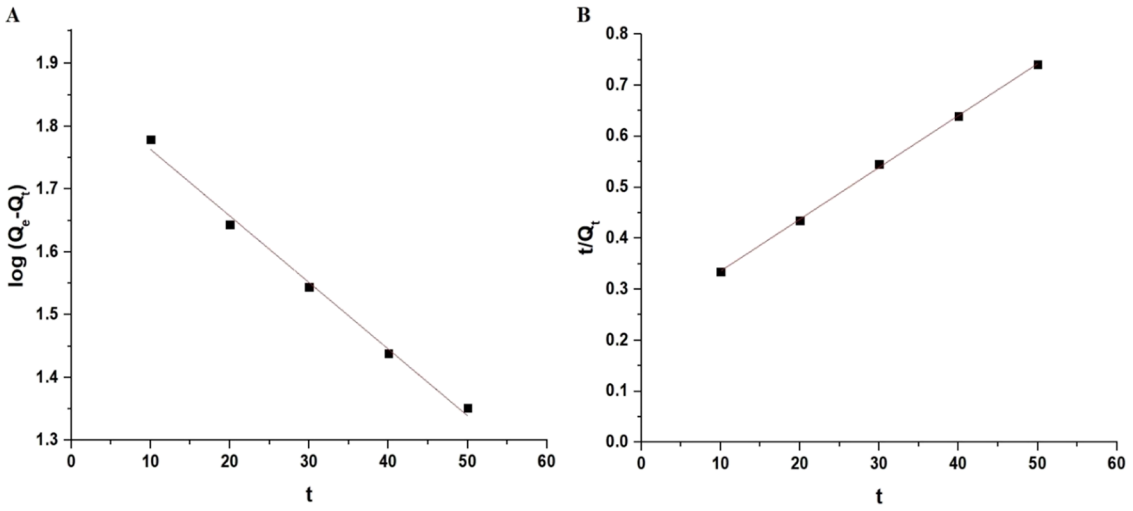

Figure 7. Pseudo-first-order (A) and pseudo-second-order (B) models.

Table 1. Constant of the Pseudo-First-Order and Pseudo-Second-Order Models

pseudo-first-order			pseudo-second-order		
K_1 (1/min)	Q_e (mg/g)	R^2	K_2 (g/mg min)	Q_e (mg/g)	R^2
0.0244	74.02	0.992	0.0004	98.43	0.999

with functional groups (OH and C═N) on the surface of the composite.

3.2.3. Influence of Temperature. The values of removal efficiency (% R) and adsorption capacity (Q) decreased when the temperature value increased from 298 to 328 K, as shown in Figure 8A,B, respectively. % R and Q (mg/g) values at temperature = 328 K are 25.00% and 30.00 mg/g, respectively. Therefore, temperature = 328 K is the best value at which the maximum possible amount of aluminum ions can be removed.

The thermodynamic parameters such as a change in free energy (ΔG°), change in the entropy (ΔS°), and change in enthalpy (ΔH°) were estimated using eqs 6–8.[1]

$$\ln K_d = \frac{\Delta S^\circ}{R} - \frac{\Delta H^\circ}{RT} \quad (6)$$

$$\Delta G^o = \Delta H^\circ - T\Delta S^\circ \quad (7)$$

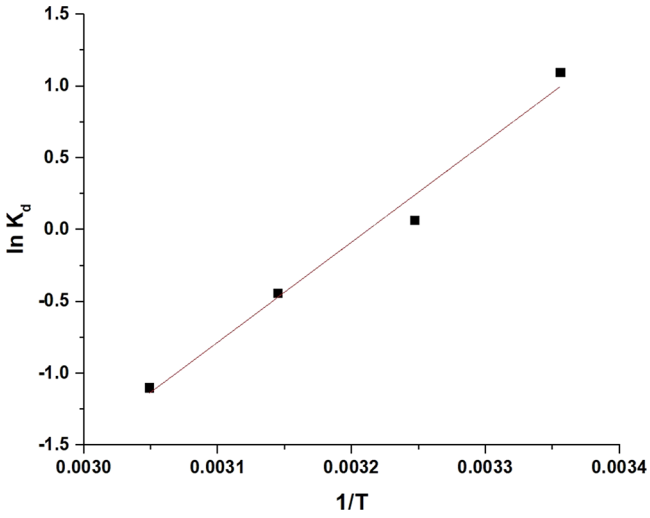

Figure 9. Plotting of lnK_d against $1/T$.

$$K_d = \frac{Q_e}{C_e} \quad (8)$$

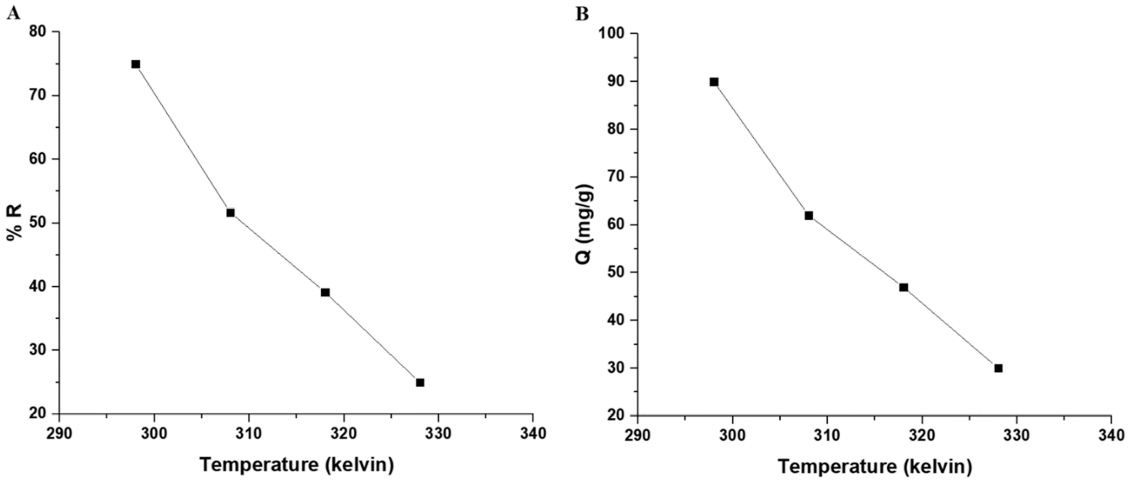

Figure 8. Effect of temperature on % R (A) and adsorption capacity (B).

https://doi.org/10.1021/acsomega.3c00413
ACS Omega 2023, 8, 15276−15287

Table 2. Thermodynamic Constants

		ΔG° (KJ/mol)			
ΔH° (KJ/mol)	ΔS° (KJ/mol K)	298	308	318	328
−58.17	0.187	−113.85	−115.72	−117.59	−119.46

Table 3. Constants of the Langmuir and Freundlich Isotherms

Langmuir			Freundlich		
K_L (L/mg)	Q_e (mg/g)	R^2	K_F ((mg/g)(L/mg)$^{1/n}$))	Q_e (mg/g)	R^2
0.665	95.06	0.999	45.21	114.09	0.586

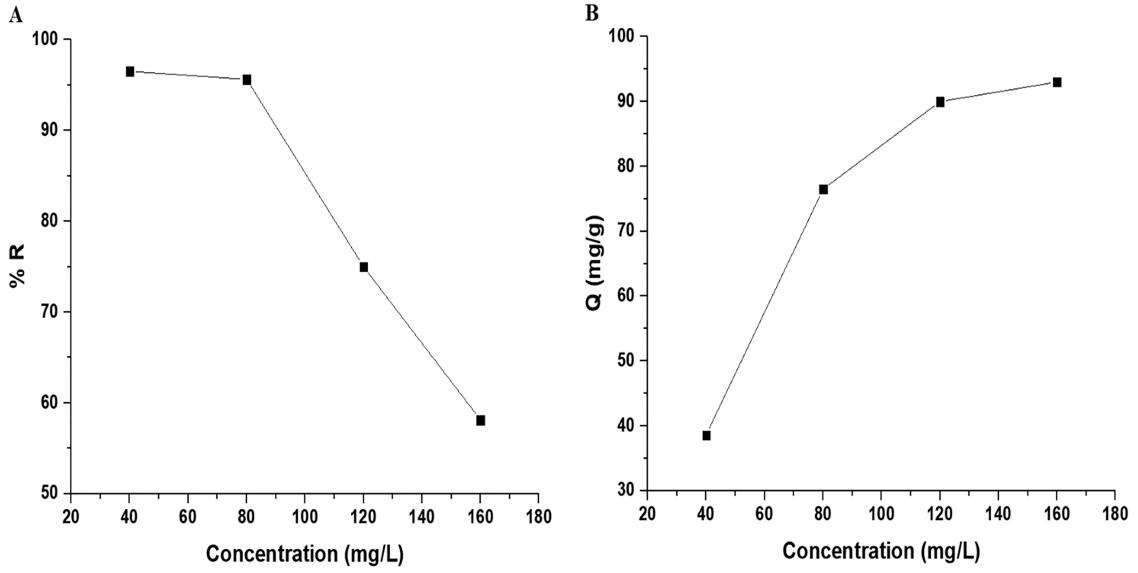

Figure 10. Effect of concentration on % R (A) and adsorption capacity (B).

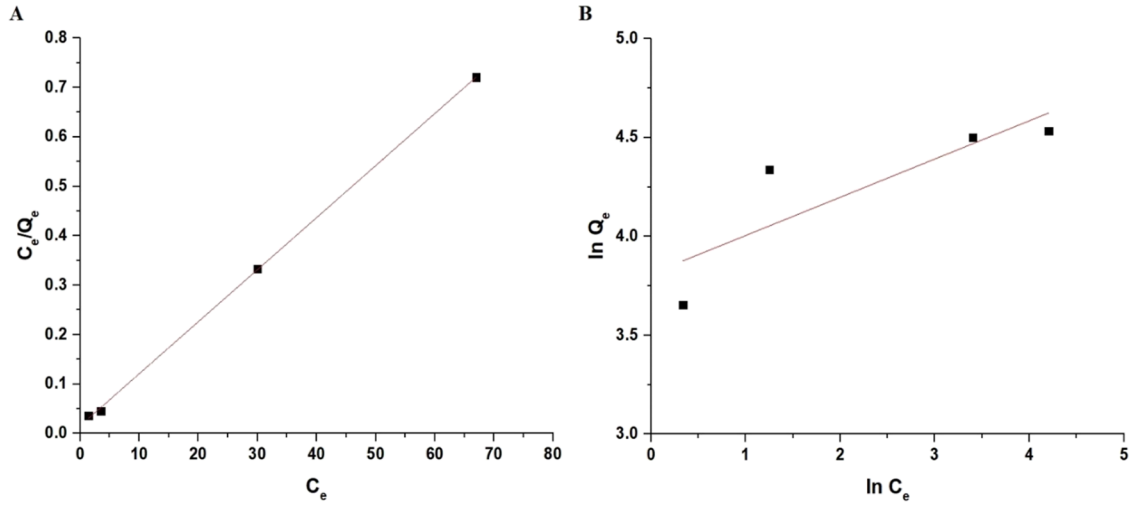

Figure 11. Langmuir (A) and Freundlich (B) isotherms.

where T represents the absolute temperature (K), while K_d represents the distribution constant (L/g). In addition, R (kJ/mol K) is the universal gas constant. Figure 9 shows the plotting of lnK_d versus $1/T$. The thermodynamic constants are tabulated in Table 2.

The negative values of ΔG° indicate that the adsorption of aluminum ions by the silica/5-chloro-8-quinolinol composite is spontaneous and thermodynamically favorable. The value of ΔH° is −58.17 KJ/mol. Hence, the value of ΔH° indicates that the adsorption of aluminum ions by the silica/5-chloro-8-quinolinol composite is exothermic and chemical. The value of ΔS° is 0.187 KJ/mol K. Hence, the adsorption of aluminum ions by the silica/5-chloro-8-quinolinol nanocomposite takes place in a disordered approach.[1]

3.2.4. Influence of Concentration. The values of removal efficiency (% R) and adsorption capacity (Q) decreased when the aluminum concentration value increased from 40 to 160 mg/L, as shown in Figure 10A,B, respectively. % R and Q (mg/

https://doi.org/10.1021/acsomega.3c00413
ACS Omega 2023, 8, 15276−15287

g) values at concentration = 160 mg/L are 58.13% and 93.00 mg/g, respectively.

To study the significant step of the removal process, experimental results were fitted with Freundlich and Langmuir isotherms, which are described by eqs 9 and 10, respectively.

$$\ln Q_e = \ln K_F + \frac{1}{n}\ln C_e \quad (9)$$

$$\frac{C_e}{Q_e} = \frac{1}{K_L Q_m} + \frac{C_e}{Q_m} \quad (10)$$

where Q_m (mg/g) is the maximal adsorption capacity of the silica/5-chloro-8-quinolinol composite. K_L (L/mg) is the Langmuir constant, whereas K_F (mg/g) $(L/mg)^{1/n}$ is the Freundlich constant. Besides, the heterogeneity constant is denoted by the fraction $1/n$. The Freundlich isotherm can be applied to compute Q_m using eq 11.[4]

$$Q_m = K_F(C_i^{1/n}) \quad (11)$$

Figure 11A,B exhibits the Langmuir and Freundlich isotherms, respectively. The constants of the Langmuir and Freundlich isotherms, as well as their correlation coefficient R^2 values, are tabulated in Table 3.

The preceding results indicated that the adsorption of aluminum ions onto the silica/5-chloro-8-quinolinol composite follows the Langmuir isotherm because the value of correlation coefficient (R^2) of the Langmuir isotherm is more than that of the Freundlich isotherm.

As clarified in Table 4, the adsorption capacity of the silica/5-chloro-8-quinolinol nanocomposite was compared to that of

Table 4. Comparative Study between the Uptake Capacity of the Silica/5-chloro-8-quinolinol Composite and that of Other Adsorbents

adsorbent	Q (mg/g)	equilibrium time (min)	ref
brilliant green-Amberlite XAD-2	10.80	10	33
poly(2-hydroxyethyl methacrylate)	17.50	60	34
tiron-modified resin	5.60	35	35
XAD-4 functionalized by salicylic acid	4.40	60	36
activated charcoal	0.360	90	37
starch	0.292	90	37
silica/5-chloro-8-quinolinol composite	95.06	60	this study

more adsorbents, for example, brilliant green-Amberlite XAD-2, poly(2-hydroxyethyl methacrylate), tiron-modified resin, XAD-4 functionalized by salicylic acid, activated charcoal, and starch.[33−37] Owing to its high adsorption capacity, the silica/5-chloro-8-quinolinol composite outperformed the aforementioned adsorbents.

3.2.5. Influence of Reusability and Desorption. Figure 12 depicts the plot of % D versus various eluting solutions. As eluting solutions, 0.40 M nitric acid, hydrochloric acid, thiourea, and EDTA disodium salt were used. Results indicated that 0.40 M EDTA disodium salt is the most effective eluting solution applied for recovering the greatest quantity of Al^{3+} ions from the silica/5-chloro-8-quinolinol nanocomposite. In addition, EDTA is the most prominent member of the ligand family. In an aqueous solution, EDTA is a hexadentate ligand

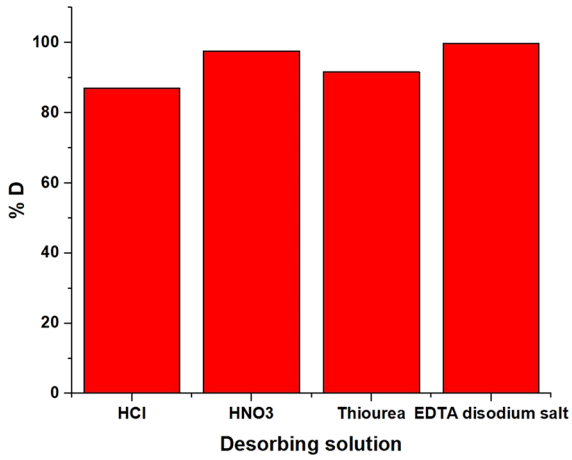

Figure 12. Plot of % D versus various desorbing solutions.

that forms very strong complexes with metal ions as reported by Khalifa et al.[24] Therefore, it is able to uptake Al^{3+} ions from the composite surface.

Figure 13 depicts the plot of % R versus the cycle number. The small decrease in % R indicates that the silica/5-chloro-8-

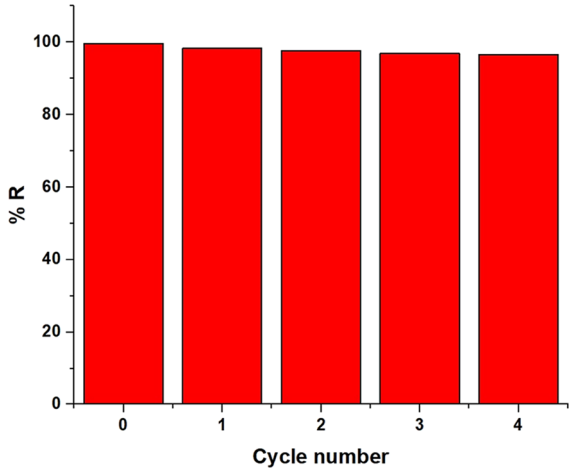

Figure 13. Plot of % R versus the cycle number.

quinolinol nanocomposite can be efficiently regenerated and reutilized for the uptake of aluminum ions from the aqueous solutions.

3.2.6. Influence of Co-Existing Ions. In order to determine the effect of some cations and anions on the elimination efficiency of aluminum ions by the existing method, the possible interfering ion was introduced at several concentrations to a 60 mL of 200 μg/L Al^{3+}solution. The elimination technique was carried out accurately as illustrated earlier, and its effectiveness was estimated. The tolerance limit was recognized as the greatest concentration of the accompanying ion resulted in a 5 percent extraction error. Table 5 clearly illustrates that the majority of coexisting ions have a rather great tolerance limit, revealing the selectivity of the procedure. Accordingly, the technique can be applied to the analysis of real samples containing various components.

3.3. Application. Prior to atomic absorption spectrometer investigation, the recommended removal procedure was applied to preconcentrate Al^{3+} ions in real water samples that were gathered from different places in Egypt (Alexandria,

https://doi.org/10.1021/acsomega.3c00413
ACS Omega 2023, 8, 15276−15287

Table 5. Effect of Interfering Ions on the Recovery of Al^{3+} Ions

diverse ion	tolerance limit (mg/L)	% R
Na^+	1000	99.30
K^+	1000	99.65
Ca^{2+}	120	95.78
Mg^{2+}	120	97.82
Ba^{2+}	120	96.78
Cd^{2+}	120	97.54
Hg^{2+}	120	96.28
Cu^{2+}	100	98.56
Zn^{2+}	80	96.72
Ni^{2+}	80	95.96
Fe^{3+}	80	96.48
HCO^{3-}	900	99.36
NO^{3-}	1000	97.89
Cl^-	900	99.57
SO_4^{2-}	900	99.23

Ras El-Bar, and Gamasah), as previously described in the experimental part. Besides, different volumes (0.2 and 0.4 mL) of a 1000 mg/L stock solution of Al^{3+} ions have been added to the water samples to evaluate the method under different conditions. Then, the adsorption and preconcentration experiments were performed for the resulting samples as previously described in the experimental part. The results of the preconcentration of Al^{3+} ions and the % recoveries for all the samples are displayed in Table S1.

% Recovery was determined by eq 12.

$$\%\text{Recovery} = \frac{\text{Found Concentration (Practically)}}{\text{Total Concentration (Theoretically)}} \times 100 \quad (12)$$

In addition, % RSD (relative standard deviation) was determined by eq 13.

$$\%\text{RSD} = \frac{\text{Standard deviation}}{\text{Mean}} \times 100 \quad (13)$$

The results confirmed that the values of % recovery were more than 97%, whereas the values of % RSD were less than 3.5%.[38] Hence, this confirms the effectiveness of the proposed method in the determination of aluminum ions in real water samples.

4. CONCLUSIONS

5-Chloro-8-quinolinol was utilized to modify the silica nanoparticles to create a new nanocomposite for the efficient elimination and preconcentration of aluminum ions from several water samples. The CHN elemental analyzer, FT-IR, XRD, SEM, TEM, and N_2 adsorption/desorption analyzer were utilized to identify the synthesized composite. The greatest uptake capacity of the synthesized nanocomposite is 95.06 mg/g. The adsorption of Al^{3+} ions onto the silica/5-chloro-8-quinolinol composite follows the Langmuir isotherm and pseudo-second-order model. The values of % recovery were more than 97%, whereas the values of % RSD were less than 3.5%.[38] Hence, this confirms the effectiveness of the proposed method in the determination of aluminum ions in real water samples.

ASSOCIATED CONTENT

Supporting Information

The Supporting Information is available free of charge at https://pubs.acs.org/doi/10.1021/acsomega.3c00413.

Determination of aluminum ions in real samples (PDF)

AUTHOR INFORMATION

Corresponding Author

Ehab A. Abdelrahman − *Department of Chemistry, College of Science, Imam Mohammad Ibn Saud Islamic University (IMSIU), Riyadh 11623, Saudi Arabia; Chemistry Department, Faculty of Science, Benha University, Benha 13518, Egypt;* orcid.org/0000-0003-2493-883X; Email: EAAAhmed@imamu.edu.sa, dr.ehabsaleh@yahoo.com

Authors

Asma S. Al-Wasidi − *Department of Chemistry, College of Science, Princess Nourah bint Abdulrahman University, Riyadh 11671, Saudi Arabia*

Hanadi A. Katouah − *Department of Chemistry, Faculty of Applied Sciences, Umm Al-Qura University, Makkah 21955, Saudi Arabia*

Fawaz A. Saad − *Department of Chemistry, Faculty of Applied Sciences, Umm Al-Qura University, Makkah 21955, Saudi Arabia*

Complete contact information is available at: https://pubs.acs.org/10.1021/acsomega.3c00413

Author Contributions

The manuscript was written through the contributions of all authors. All authors have given approval to the final version of the manuscript.

Notes

The authors declare no competing financial interest.

ACKNOWLEDGMENTS

The authors are grateful to Princess Nourah bint Abdulrahman University, Riyadh, Saudi Arabia for funding this work through Researchers Supporting Project number (PNURSP2023R35).

REFERENCES

(1) Ren, Z.; Wang, L.; Li, Y.; Zha, J.; Tian, G.; Wang, F.; Zhang, H.; Liang, J. Synthesis of Zeolites by In-Situ Conversion of Geopolymers and Their Performance of Heavy Metal Ion Removal in Wastewater: A Review. *J. Clean. Prod.* **2022**, *349*, No. 131441.

(2) Li, M.; Kuang, S.; Kang, Y.; Ma, H.; Dong, J.; Guo, Z. Recent Advances in Application of Iron-Manganese Oxide Nanomaterials for Removal of Heavy Metals in the Aquatic Environment. *Sci. Total Environ.* **2022**, *819*, No. 153157.

(3) Li, W.; Guo, J.; Du, H.; Wang, D.; Cao, J.; Wang, Z. Selective Removal of Aluminum Ions from Rare Earth Solutions by Using Ion-Imprinted Polymers. *Sep. Purif. Technol.* **2022**, *286*, No. 120486.

(4) Rashno, M.; Gholipour, P.; Salehi, I.; Komaki, A.; Rashidi, K.; Esmaeil Khoshnam, S.; Ghaderi, S. P-Coumaric Acid Mitigates Passive Avoidance Memory and Hippocampal Synaptic Plasticity Impairments in Aluminum Chloride-Induced Alzheimer's Disease Rat Model. *J. Funct. Foods* **2022**, *94*, No. 105117.

(5) Forsido, T. T.; McCrindle, R. I.; Maree, J.; Monyatsi, L. Removal of Al, Ba and Mg from Industrial Wastewater Using EAFDS and Lime. *Appl. Water Sci.* **2020**, *10*, 157.

(6) Safavi, A.; Momeni, S.; Saghir, N. Efficient Preconcentration and Determination of Traces of Aluminum Ion Using Silica-Bonded Glycerol Sorbent. *J. Hazard. Mater.* **2009**, *162*, 333−337.
(7) Xia, L.; Hu, B.; Jiang, Z.; Wu, Y.; Li, L.; Chen, R. 8-Hydroxyquinoline-Chloroform Single Drop Microextraction and Electrothermal Vaporization ICP-MS for the Fractionation of Aluminium in Natural Waters and Drinks. *J. Anal. At. Spectrom.* **2005**, *20*, 441−446.
(8) Sun, M.; Wu, Q. Determination of Ultra-Trace Aluminum in Human Albumin by Cloud Point Extraction and Graphite Furnace Atomic Absorption Spectrometry. *J. Hazard. Mater.* **2010**, *176*, 901−905.
(9) Bulut, V. N.; Arslan, D.; Ozdes, D.; Soylak, M.; Tufekci, M. Preconcentration, Separation and Spectrophotometric Determination of Aluminium(III) in Water Samples and Dialysis Concentrates at Trace Levels with 8-Hydroxyquinoline-Cobalt(II) Coprecipitation System. *J. Hazard. Mater.* **2010**, *182*, 331−336.
(10) Ozdemir, S.; Turkan, Z.; Kilinc, E.; Bayat, R.; Soylak, M.; Sen, F. Preconcentrations of Cu (II) and Mn (II) by Magnetic Solid-Phase Extraction on Bacillus Cereus Loaded γ-Fe_2O_3 Nanomaterials. *Environ. Res.* **2022**, *209*, No. 112766.
(11) Ates, N.; Basak, A. Selective Removal of Aluminum, Nickel and Chromium Ions by Polymeric Resins and Natural Zeolite from Anodic Plating Wastewater. *Int. J. Environ. Health Res.* **2021**, *31*, 102−119.
(12) Karpinsky, M. M.; Arnold, A. M.; Lee, J.; Jasper, G.; Bockstaller, M. R.; Sydlik, S. A.; Zovinka, E. P. Acid Mine Drainage Remediation: Aluminum Chelation Using Functional Graphenic Materials. *ACS Appl. Mater. Interfaces* **2020**, *12*, 32642−32648.
(13) Popugaeva, D.; Manoli, K.; Kreyman, K.; Ray, A. K. Removal of Aluminum from Aqueous Solution by Adsorption on Montmorillonite K10, TiO_2, and SiO_2: Kinetics, Isotherms, and Effect of Ions. *Adsorption* **2019**, *25*, 1575−1583.
(14) Corral-Bobadilla, M.; González-Marcos, A.; Alba-Elías, F.; de Santo, D.; Domingo, E. Valorization of Bio-Waste for the Removal of Aluminum from Industrial Wastewater. *J. Clean. Prod.* **2020**, *264*, No. 121608.
(15) Delgadillo-Velasco, L.; Hernández-Montoya, V.; Ramírez-Montoya, L. A.; Montes-Morán, M. A.; del Rosario Moreno-Virgen, M.; Rangel-Vázquez, N. A. Removal of Phosphate and Aluminum from Water in Single and Binary Systems Using Iron-Modified Carbons. *J. Mol. Liq.* **2021**, *323*, No. 114586.
(16) Mortada, W. I.; Kenawy, I. M. M.; Abou El-Reash, Y. G.; Mousa, A. A. Microwave Assisted Modification of Cellulose by Gallic Acid and Its Application for Removal of Aluminium from Real Samples. *Int. J. Biol. Macromol.* **2017**, *101*, 490−501.
(17) Lobo-Recio, M. Á.; Rodrigues, C.; Custódio Jeremias, T.; Lapolli, F. R.; Padilla, I.; López-Delgado, A. Highly Efficient Removal of Aluminum, Iron, and Manganese Ions Using Linde Type-A Zeolite Obtained from Hazardous Waste. *Chemosphere* **2021**, *267*, No. 128919.
(18) Saleh, T. A.; Tuzen, M.; Sari, A. Magnetic Activated Carbon Loaded with Tungsten Oxide Nanoparticles for Aluminum Removal from Waters. *J. Environ. Chem. Eng.* **2017**, *5*, 2853−2860.
(19) Abdelrahman, E. A.; Abou El-Reash, Y. G.; Youssef, H. M.; Kotp, Y. H.; Hegazey, R. M. Utilization of Rice Husk and Waste Aluminum Cans for the Synthesis of Some Nanosized Zeolite, Zeolite/Zeolite, and Geopolymer/Zeolite Products for the Efficient Removal of Co(II), Cu(II), and Zn(II) Ions from Aqueous Media. *J. Hazard. Mater.* **2021**, *401*, No. 123813.
(20) Abdelrahman, E. A.; Alharbi, A.; Subaihi, A.; Hameed, A. M.; Almutairi, M. A.; Algethami, F. K.; Youssef, H. M. Facile Fabrication of Novel Analcime/Sodium Aluminum Silicate Hydrate and Zeolite Y/Faujasite Mesoporous Nanocomposites for Efficient Removal of Cu(II) and Pb(II) Ions from Aqueous Media. *J. Mater. Res. Technol.* **2020**, *9*, 7900−7914.
(21) Abdelrahman, E. A.; Hegazey, R. M. Exploitation of Egyptian Insecticide Cans in the Fabrication of Si/Fe Nanostructures and Their Chitosan Polymer Composites for the Removal of Ni(II), Cu(II), and Zn(II) Ions from Aqueous Solutions. *Compos. Part B Eng.* **2019**, *166*, 382−400.
(22) Abdelrahman, E. A.; Hegazey, R. M. Utilization of Waste Aluminum Cans in the Fabrication of Hydroxysodalite Nanoparticles and Their Chitosan Biopolymer Composites for the Removal of Ni(II) and Pb(II) Ions from Aqueous Solutions: Kinetic, Equilibrium, and Reusability Studies. *Microchem. J.* **2019**, *145*, 18−25.
(23) Bulgariu, L.; Bulgariu, D. Functionalized soy waste biomass - A novel environmental-friendly biosorbent for the removal of heavy metals from aqueous solution. *J. Clean. Prod.* **2018**, *197*, 875−885.
(24) Khalifa, M. E.; Abdelrahman, E. A.; Hassanien, M. M.; Ibrahim, W. A. Application of Mesoporous Silica Nanoparticles Modified with Dibenzoylmethane as a Novel Composite for Efficient Removal of Cd(II), Hg(II), and Cu(II) Ions from Aqueous Media. *J. Inorg. Organomet. Polym. Mater.* **2020**, *30*, 2182−2196.
(25) Al-Wasidi, A. S.; Naglah, A. M.; Saad, F. A.; Abdelrahman, E. A. Modification of Silica Nanoparticles with 4,6-Diacetylresorcinol as a Novel Composite for the Efficient Removal of Pb(II), Cu(II), Co(II), and Ni(II) Ions from Aqueous Media. *J. Inorg. Organomet. Polym. Mater.* **2022**, *32*, 2332−2344.
(26) Soltani, R.; Dinari, M.; Mohammadnezhad, G. Ultrasonic-Assisted Synthesis of Novel Nanocomposite of Poly(Vinyl Alcohol) and Amino-Modified MCM-41: A Green Adsorbent for Cd(II) Removal. *Ultrason. Sonochem.* **2018**, *40*, 533−542.
(27) Mallakpour, S.; Dinari, M. Investigating the Nanostructure and Thermal Properties of Chiral Poly(Amide-Imide)/Al_2O_3 Compatibilized with 3-Aminopropyltriethoxysilane. *Mater. Res. Bull.* **2013**, *48*, 3865−3872.
(28) Cui, Y.; Chang, X.; Zhu, X.; Luo, H.; Hu, Z.; Zou, X.; He, Q. Chemically Modified Silica Gel with P-Dimethylaminobenzaldehyde for Selective Solid-Phase Extraction and Preconcentration of Cr(III), Cu(II), Ni(II), Pb(II) and Zn(II) by ICP-OES. *Microchem. J.* **2007**, *87*, 20−26.
(29) Fan, J.; Wu, C.; Wei, Y.; Peng, C.; Peng, P. Preparation of Xylenol Orange Functionalized Silica Gel as a Selective Solid Phase Extractor and Its Application for Preconcentration-Separation of Mercury from Waters. *J. Hazard. Mater.* **2007**, *145*, 323−330.
(30) Xu, Y.; Wang, C.; Zhou, G.; Wu, Y.; Chen, J. Improving the Controlled Release of Water-Insoluble Emodin from Amino-Functionalized Mesoporous Silica. *Appl. Surf. Sci.* **2012**, *258*, 6366−6372.
(31) Xu, Y. Q.; Zhou, G. W.; Wu, C. C.; Li, T. D.; Song, H. Bin Improving Adsorption and Activation of the Lipase Immobilized in Amino-Functionalized Ordered Mesoporous SBA-15. *Solid State Sci.* **2011**, *13*, 867−874.
(32) Kenawy, I. M. M.; Abou El-Reash, Y. G.; Hassanien, M. M.; Alnagar, N. R.; Mortada, W. I. Use of Microwave Irradiation for Modification of Mesoporous Silica Nanoparticles by Thioglycolic Acid for Removal of Cadmium and Mercury. *Microporous Mesoporous Mater.* **2018**, *258*, 217−227.
(33) Ahmad Panahi, H.; Feizbakhsh, A.; Riyasati, S.; Moniri, E.; Nezhati, M. N.; Galaev, I. Y. Preconcentration and Determination of Aluminum in Water Samples by Inductively Coupled Plasma-Atomic Emission Spectroscopy with Brilliant Green-Based Anion-Exchange Solid-Phase Extraction Support. *Desalin. Water Treat.* **2015**, *53*, 1902−1908.
(34) Yavuz, H.; Say, R.; Andaç, M.; Bayraktar, N.; Denizli, A. Performance of Dye-Affinity Beads for Aluminium Removal in Magnetically Stabilized Fluidized Bed. *Biomagn. Res. Technol.* **2004**, *2*, 5.
(35) Luo, M.; Bi, S. Solid Phase Extraction-Spectrophotometric Determination of Dissolved Aluminum in Soil Extracts and Ground Waters. *J. Inorg. Biochem.* **2003**, *97*, 173−178.
(36) Vanloot, P.; Boudenne, J. L.; Brach-Papa, C.; Sergent, M.; Coulomb, B. An Experimental Design to Optimize the Flow Extraction Parameters for the Selective Removal of Fe(III) and Al(III) in Aqueous Samples Using Salicylic Acid Grafted on Amberlite XAD-4 and Final Determination by GF-AAS. *J. Hazard. Mater.* **2007**, *147*, 463−470.

https://doi.org/10.1021/acsomega.3c00413
ACS Omega 2023, 8, 15276−15287

(37) Choksi, P. M.; Joshi, V. Y. Adsorption Kinetic Study for the Removal of Nickel (II) and Aluminum (III) from an Aqueous Solution by Natural Adsorbents. *Desalination* **2007**, *208*, 216−231.
(38) Al-Wasidi, A. S.; AlSalem, H. S.; Alshalawi, A. F.; Naglah, A. M.; Al-Anwar, A.; Abdelrahman, E. A. Facile synthesis of a novel nanocomposite for determination of mercury and copper ions in food and water samples. *Arab. J. Chem.* **2022**, *15*, No. 104113.

https://doi.org/10.1021/acsomega.3c00413
ACS Omega 2023, 8, 15276−15287